Reprinted from

Ninth International Symposium

Machine Processing of

Remotely Sensed Data

with special emphasis on

Natural Resources Evaluation

June 21-23, 1983

Proceedings

Purdue University
The Laboratory for Applications of Remote Sensing
West Lafayette, Indiana 47907 USA

LABORATORY SIMULATED MICROWAVE REMOTE SENSING STUDIES

K.K. JHA, K.P. SINGH, R.N. SINGH

Banaras Hindu University
Varanasi, India

ABSTRACT

Using X-band (9.52 GHz) bistatic scatterometer system, measurements were performed on various modelled targets such as dry and smooth earth surface, moist earth surface, rough earth surface, stratified earth surface and the smooth earth surface embeded with iron balls of size 1/8". Angular variations of forward as well as backward scattering cross-sections in both the polarizations (VV and HH) were measured. From the measured forward scattered data, the emissivity and brightness temperature have been calculated following reciprocity theorem and the results were compared with the results obtained by other workers. The importance of laboratory and field measurements for signature study and its application in remote sensing has been discussed.

I. INTRODUCTION

The emergence of remote sensing as a tool for mapping earth's surface and studying the structure and composition of its interior has revived various types of laboratory measurements and theoretical studies. Detailed knowledge of electromagnetic response in the extended frequency range help the investigators to recognise the target exactly in the same way as the bank agent recognises the payee by his signature. This analogy has been aptly used and the science of target response is known as remote sensing signature analysis. The successful interpretation of microwave radiometer data obtained from remote sensing satellite depends mainly on the extensive knowledge of microwave response of various types of earth forming materials, their composition, moisture content, surface roughness, vegetation cover, look angle response, frequency, polarization and integrated atmospheric attenuation. Using scatterometer system, airborne and spaceborne sensors extensive measurement of soil moisture has been carried out by many workers and is very well documented[1]. The application of remotely determined soil moisture range from agriculture (in which moisture is related to crop growth) to civil works (where moisture is a major factor in slope stability studies because it increases weight, reduces shearing resistance, and significantly reduces shear strengths of materials[2]. Soil moisture plays an important role in number of disciplines including hydrology and meteorology[3] for these and other applications the knowledge of soil moisture is essential. Using bistatic scatterometer system in the X-band (9.52 GHz), we have highlighted the various parameters, such as, soil moisture, surface roughness, dielectric constant, fluctuation and earth surface stratification which affect the microwave sensor response. It has been shown that around Brewster's angle the vertical polarization does not deciphere clearly the dry ground from the moist ground. Although the shifts in Brewster's angle is measurable. Basically, in the present experiment a model tank of size 6'x4'x1/2' was filled with dry soil and measurements were carried out for various modelling. The stratification was limited within the skin depth as seen by the incident X-band microwave. Three layer stratification and various combinations of sand silt stone, sand-silt-metal plate-stone were used in the experiment. The various efforts of mocked up earth's surface study was made in the recent past[4,5,6]. It has been found that Brewster's angle was changed with the nature of stratification. The stratified layer's study has great relevance to practical situation faced in practice. The earth's crust is, in general, stratified with various layers of different composition, structure and thickness. Thus, these measured results confirms that stratification changes the reflectivity and its corresponding brightness temperature from one sequence to another significantly. The open field surfaces satisfy the Rayleigh's criterian and make the surface slightly rough having certain height distributions, in such cases we have measured the backscattering cross-section. The measurements also show how the plane surface Fresnel's reflection coefficient is modified due to surface roughness. The backscattering cross-section (σ°) measurement for slightly rough surface with moisture shows that for both VV and HH polarizations, the value of σ° at lower angle is larger and decreases monotonically. Further, the addition of moisture increases the values of σ°. The results were found in good agreement with the reported results. Similar scattering measurements have been carried out by creating the dielectric constant fluctuations. Some scattering pattern were created by putting rows of iron balls (size 1/3") on the plane homogeneous sand surfaces which produces dielectric constant fluctuations. The look angle variation of reflectivity and backscattering cross-section was measured for iron balls parallel to trans-receiver line and that of perpendicular to trans-receiver line. Some oscillation was observed due to interference of deffracted power. When the spacing between the rows were less oscillations were found to be minimum. These measurements with surface undulation and dielectric embeding provide the basic understanding of some of the natural targets. The effort made is no doubt meagre but we found it very difficult to interpret the observed variations. We feel that these measured data's from model experiments are helpful in analysing and interpreting the remote sensing data obtained by distant sensors.

II. BISTATIC SCATTEROMETER SYSTEM (DESCRIPTION)

Ground based scatterometer has been used as an auxiliary source of information for interpreting airborne or spaceborne sensors data. Scatterometer measures the reflected or scattered energy from the target surface (or sometime from volume). An active scatterometer system measures the reflected or scattered wave generated by the active sensor itself. Scatterometry provides useful signatures only if its operation is limited for short range, such as from platform, bridge, building, towers etc. then it provides so called ground truth. It is particularly useful in the study of moisture variation in soil and vegetation as well as in the study of vegetation growth cycle, and laboratory simulated wave tank etc. By using spaceborne sensors, frequency variation characteristic (i.e. measurements in extended frequency range) for various polarization combination and wide angular response is not possible, while scatterometer can be used for extended frequency range, for various polarization combination and it can operate for wide angle also. One of the major drawback of scatterometer (ground based) is that, due to its limited beamwidth the foot print of the antenna used is smaller in size and thus it can not be used to obtain enough independent samples of the (more or less) Rayleigh type[7], whereas antenna used in airborne or spaceborne sensors covers a large area and provide information for significant number of independent samples. Thus, by using scatterometer system, informations are gathered in an environment whereas many parameters as possible were under control.

By using bistatic scatterometer system, two types of measurements have been carried out:

1. Forward scattering or reflectivity measurement
2. Backward scattering or back scattered cross-section measurement.

II.a. Description of Equipment set up and Measurement Procedure

Figure 1 illustrates the schematic representation of the equipment used in this experiment. The waterproof holding tank, in which the target medium was placed, was constructed of perspex ($\epsilon_r = 2.14$) having dimensions 6'x4' wide and 1.5' deep. For reflectivity measurement two identical pyramidal horn antennas one acting as the transmitter and the other as the receiver having half power beamwidth 19° and 22° in E and H-plane respectively with a gain of 26 dB, operating at frequency 9.52 GHz were mounted on a specially designed portable stand on either side of the model tank along a straight line. While in the case of backscattering cross-section measurement the two horn antennas were mounted on the same stand. The height and look angle of the horn mounted on this stand can be varied. The height and look angle can be read from the graduated circular scales and pointer provided on the stand. The polarization of the radiated signal is changed by using 90° E-H twist. The size of the tank, the height of the transmitter and receiver stands, and their distances allow a practical variation of look angle between 20° to 75°. The angles of incidence of microwave signal are systematically changed and the specularly reflected or scattered component of the signal from the center of the model target are located. Best care has been taken to avoid stray reflection under experimental conditions by putting a 30 dB microwave absorber to the exposed part. The antennas were placed always 1 meter away in the far field region from the center of the target to minimize near field interaction.

The operation of the equipment can be described as follows:

An amplitude modulated (AM) signal of frequency 9.52 GHz generated by the Klystron source, was fed through variable attenuator, 20 dB directional coupler and then on to the transmitting antenna, whereby it is radiated towards the target. After interaction with the target, located in the far field, an amount of signal returns towards the receiving antenna, which is subsequently demodulated by the rectifying diode detector and then amplified by the tuned audio amplifier. The operation of diode detector is assured to be in square-law region (i.e. the square of the output detector voltage is directly proportional to the input power supplied to it) by adjusting the transmitted power at low level. The overall system was calibrated by noting the signal returned from an alluminium plate placed on the top of the target surface. To assure that the transmitted power is low enough for its operation in square law region, a known amount of loss in dB was introduced through the attenuator in the transmitting arm. It was observed that the meter connected to the receiving arm displays same amount of introduced loss. This ensures the detector's operation in the square-law region. After this important check measurements were carried out for all possible angle keeping the alluminium plate on the target. Next, the plate was removed and then the repeated angular measurements for the target was carried out. Apart from this check, the equipment was frequently monostatically calibrated against a corner reflector with known properties, and bistatically calibrated against the direct view of the transmitter and receiver. The calibration of the system was checked at an interval of 30 minutes during the experiment. The following expressions were used:

For reflectivity measurement[1]

$$r = |R|^2 = \frac{P_R \times 4\pi (R_1 + R_2)^2}{P_T\ G_T\ \underline{k} A_o\ X} \qquad (1)$$

where $X = \exp(-2\sigma^2 k^2 \cos^2\theta) \simeq 1$ is known as variance of surface height

$k = 2\pi/\lambda$ where λ is operating wavelength

P_R = received power

P_T = transmitted power

$\underline{k}$ = a factor defined by the ratio of capture area A to the aperture area A_o of the receiving horn

R_1 and R_2 = distances of the transmitting and receiving horn respectively to the central point of the target

and G_T = gain of the transmitting horn.

The reflectivity data obtained by using equation (1) was compared with the reported formula[5]. As has been described in the measurement procedure, let m_p be the measured output of audio amplifier in dB with alluminium plate on the target surface and m_{NP} be the measured output of audio amplifier in dB with no alluminium plate (i.e., power reflected from the target surface) then,

$$m_p - m_{NP} = 10 \log r \qquad (2)$$

$$\text{or } r = 10^{1/10\,(m_p - m_{NP})} \qquad (3)$$

where r is the target reflectivity.

The data obtained by using equations (1) and (3) are similar upto three decimal places.

For backscattering cross-section measurement[1]

$$10 \log \sigma^\circ = 10 \log \sigma^\circ_{srt} + 10 \log P_s - 10 \log P_{dlt} + 10 \log P_{dll} - 10 \log P_{srt} + 40 \log R_t - 40 \log R_c - 10 \log A_{ill}. \qquad (4)$$

where σ° = differential scattering cross-section per unit area

srt = standard radar target (corner reflector)

P_s = received power from surface

P_{dlt} = detected power through delay line (in the absence of corner reflector)

P_{dll} = detected power through delay line (in the presence of corner reflector)

P_{srt} = power received from corner reflector

R_t = range to target

R_c = range to corner reflector

A_{ill} = illuminated area.

III. RESULTS AND DISCUSSION

Using bistatic scatterometer system, the reflectivity of a target of varying nature was measured. The target surfaces was specially prepared for the measurement. The surface roughness was kept unity (smooth). The site under study was filled with water, such that the moisture content of the surface was constantly measured and monitored with various states of drying of the soil surface. The moisture content was measured by taking the soil samples from the subsurface layer. The experiment was conducted in the month of June (in India particularly in Varanasi, the temperature is high enough in May and June). Therefore, the moisture percentage given can be considered as average moisture content with an error of ±2%. The variation of emissivity and corresponding brightness temperature follows from the reciprocity relation as

$$e = (1 - r) \quad (5)$$

where e is the emissivity

$$T_B = e\,T_s + r\,T_{sky} = (1-r)\,T_s + r\,T_{sky} \quad (6)$$

where T_B is the brightness temperature and

T_s is the surface temperature of the target.

In this discussion due to short range, contribution of the sky radiance T_{sky} will be neglected. The angular variation of emissivity and brightness temperature as a function of moisture content is just opposite of what is observed in the case of reflectivity. From the reflectivity data we have computed the corresponding brightness temperature of the target. Figure 2 and 3 show the angular variation of brightness temperature as a function of moisture content. From figures we note that for vertical polarization at 25° look angle, the brightness temperature for dry ground is ~ 293°K and for ground with 30% moisture, ~ 204°K. Thus, the moisture content decreases the brightness temperature by 90°K. For horizontal polarization the brightness temperature value was found to be ~ 265°K for dry ground, and ~ 168°K for moist ground with 30% moisture content. The difference in both the polarization is around 90°K. These results are in good agreement with the reported results[3,8,9]. The figure depicts the moisture variation from 5% to 30% at an interval of 5%. Figure 4 shows the dependence of emissivity with moisture content at angles 35°, 59°, 63° and 68° for vertical polarization and Figure 5 shows the dependence of emissivity at angles 25° and 45° for both the polarizations (VV and HH). Here we see that the emissivity decreases with moisture content for look angles 25°, 35° and 45°, while the data computed for 59°, 63° and 68° shows a somewhat straight line behaviour. The probable explanation in this respect is that around Brewster's angle the major portion of power is transmitted in the soil medium and less is returned to the receiver. Therefore, the use of vertical polarization for sensing soil moisture near Brewster's angle is not very helpful. Around this angle the vertical polarization is unable to identify moist ground from dry ground. Thus, for airborne operation of vertical polarization the operation should be on lower angles ($< 50°$) while horizontal polarization is equally applicable at all angles of incidence.

The effect of surface roughness is to decrease the reflectivity of the surface and thus to increase its emissivity. The brightness temperature in this case is related with emissivity as

$$T_B = (e_o \pm \Delta e)\,T_s \quad (7)$$

Let e_o be the emissivity of the plane and dry ground. The effect of surface roughness and increase or decrease of moisture content is to increase or decrease of the emissivity (Δe), which results in corresponding changes in the brightness temperature. The roughness of the surface decreases the planar reflectivity according to the relation

$$r_h = r_o\,e^{-h} \quad (8)$$

This shows that the emissivity and brightness temperature are affected by surface roughness. The backscattered signals are small enough and therefore, most of the time these signals are smaller than the background noise. Figure 6 and 7 depicts the angular variation of backscattering coefficient (σ°) as a function of moisture content and surface roughness. From figures it is clear that roughening the surface increases the backscattering coefficient, σ°. This is equally true for both the polarization combinations. The following conclusions have been drawn from the experimentally observed data. In Figure 6 when the RMS height is 3 cm nearly of the order of operating wavelength curves for 5% and 10% moisture for both VV and HH-polarizations exhibit slow and monotonic decays (i.e., the total dynamic range between 25° and 73° is ~ 8 dB). The angular responses of the 25% and 30% moisture content appear to decrease slowly and tends towards saturation at larger angles (the total dynamic range between look angles of 25° to 73° comes to around 20 dB). In Figure 7, when the RMS height is 7 cm $\gg\lambda$ the curves for 5%, 20% and 30% moisture content gives the similar behaviour. The total dynamic range between angle 25° and 73° is found to be 5 dB and also when we compare the two figures we find that the magnitude obtained with 7 cms RMS height is less than the magnitude obtained with 3 cm RMS height. We notice that, as the moisture content increases, the backscattering coefficient increases for lower angles, after 55° angles of incidence, the effect of moisture is not so prominent (i.e., all the curves decreases monotonically). The probable explanation for this is that, the increase in moisture content not only influences the dielectric properties of the soil, but it also causes the surface texture to appear smoother to the incident wave at larger angles of incidence. Thus, it decreases the separation between the curves at higher angles. This situation is equally true for $\lambda \sim h$ as well as for $\lambda < h$. We have compared these backscattering variation with look angle from the result of other workers[10,11] and have found that the nature of variation is nearly same (due to lack of system sensitivity we can not claim the magnitude).

In the case of model tank experiment with different settings of iron balls, we illustrate the look angle variation of the emissivity only. The reflectivity variation is implied and the brightness temperature follows from these curves. Figure 8 shows the angular variation of emissivity for two types of iron ball patterns placed over the dry and smooth sand surface. The measurement procedure is similar to that described earlier. The iron balls were set on the surface with rows parallel to trans-receive line as well as perpendicular to trans-receive line. Three sets of observations were made with different spacings between the rows. The balls in the rows were placed closed to each other. The look angle variation of emissivity derived from measured reflectivity shows quite interesting features. This variation shows some oscillations which is characteristic of iron balls setting. The response of VV and HH-polarization show somewhat different variations. The VV-polarization shows large emissivity and small variation. However, the look angle variation of HH-polarization falls rapidly with increasing look angle but shows large amplitude periodic variations. The probable explanation of these observation is not yet arrived at. What seems certain is that the E vector parallel to iron balls rows induces more current and hence reradiates efficiently which amounts to better reflected or scattered power. The reflected or scattered power from different rows when received at distant point bear some phase relation which keeps on changing with changing look angle. This situation results in constructive and destructive interference giving rise to undulations in the emissivity. For orthogonal row system the effect is less pronounced. The only inference which could be made from these observations is that the embeded metallic substance may give specific response to remote sensing electromagnetic waves. The X-band microwaves can penetrate to smaller depth but the low frequency signals are capable of penetrating to larger depths and revealing the presence of embeded materials. Further, the orientation, size, shape and separation of scatterers give rise to characteristic reflectivity response which can be interpreted as interference pattern of signal reflected or scattered from two or more than two parallel or perpendicular rows. The response of each pattern of ball settings gives rise to its own undulation which of course varies only slightly from one to another. Figure 9 shows the backscattering cross-section (σ^o) value calculated for the three patterns of iron ball lines. Since maximum power is scattered in the forward direction when the electric field is parallel to row direction, less power is scattered in the backward direction and this gives a lesser value of σ^o. While the reverse is true when we consider that electric field is perpendicular to row direction. The backscattering is prominent in this later case.

Most geologic media are not homogeneous and possesses many random inhomogeneities in their bulk. For a particular frequency, dielectric fluctuation due to the inhomogeneities have a small effect on the medium and the medium appears electromagnetically homogeneous. The stratified layers under dry conditions are assumed to be in thermal equilibrium with the surrounding temperature. In the case of moisture containing wet sample the physical temperature was found to be 1-2°C smaller than the surrounding temperature. Using computed emissivities the brightness temperature variation with look angles have been computed and shown in Figure 10. The brightness temperature for two polarizations are found to change significantly with look angle variations. The maximum brightness temperature is found to be around 290°K for vertical polarization. The brightness temperature is found to decrease by 25°K for moisture content of 15 per cent by weight. In the case of horizontal polarization, the brightness temperature is maximum at lower look angles and is higher for dry sample and decreases for the wet sample. The horizontal polarization at lower angles is more sensitive to moisture content and depicts a variation of 70°K for 15 per cent moisture content by weight. This is quite understandable because of the bulk effect of the earth's surface which results in a cumulative radiation. The bulk effect has been crudely estimated by varying the thickness of the mocked-up layers. The comparison of results from actual surfaces and mocked-up surfaces may provide better insight in the interpretation of satellite data.

IV. CONCLUSIONS

The laboratory measurements provide realistic signature of the mocked-up subsurface composition, stratification and moisture content, which is found to be polarization dependent. The signature of known samples and their bulk effect are important in interpreting the satellite data and in obtaining physical parameters closer to the ground truths. The reliable and meaningful correlation of the measured data with satellite measured brightness temperature can be developed by carrying out extensive laboratory and field measurements using ground truths and the corresponding sky temperature in various known conditions. Such a study would enable us to develop empirical relationships and correction factors which may prove very useful in interpreting the satellite data.

REFERENCES

1. Jha, K.K., Laboratory simulated microwave remote sensing studies. Ph.D. Thesis, Banaras Hindu University, INDIA (1982).

2. Greeley, R., Blanchard, M.B., and Gelnett, R., Geol. Soc. Amer., 6, 184 (1974).

3. Schmugge, T.J., Photogrammetric engineering and remote sensing, 46, 495 (1980).

4. Blinn, J.C., III, Conel, J.E. and Quade, J.G., J. Geophy. Res., 77, 4366 (1972).

5. Caulfield, M.S., Radiative transfer theory applied to remote sensing of scattering media, M.S. Dissertation, Massachusets Inst. of Tech. (1978).

6. Jha, K.K., Singh, K.P. and Singh, R.N., Microwave response of earth's surface constituents and its relevance to remote sensing application, URSI Commission-F Symp., University of Kansas, U.S.A., Jan. 5-8 (1981).

7. Reeves, R.G., Manual of remote sensing, American Society of Photogrammetry, Falls Church, Virginia (1975).

8. Cihlar, J. and Ulaby, F.T., RSL Tech. Rept. 177-47, Univ. of Kansas Center for Res. Inc., Lawrence, Kansas (1974).

9. Newton, R.W., Tech. Rept. RSC-81, Texas A & M Univ., College Station, Texas (1977).

10. Cosgriff, R.L., Peake, W.H. and Taylor, R.C., Terrain Handbook II, Eng. Exp. Sta., Ohio State Univ. (1960).

11. Ulaby, F.T., IEEE Trans. on Ant. Prop. AP-22, 257 (1974).

Prof. Rama N. Singh was born in U.P., India where he obtained his B.Sc., M.Sc. and Ph.D. degrees in Physics from Banaras Hindu University. He is presently a Professor of Physics in Applied Physics Section, I.T., B.H.U. His research area includes, Ionospheric Physics, Magnetospheric Physics, Space Physics, Astrophysics, Plasma Physics, Solid State Plasmas and Remote Sensing. He has published 125 research papers in various Indian and foreign journals and 16 students obtained Ph.D. degree under his supervision. He is an author of Electromagnetic Waves and Fields, Graduate level text book.

Dr. Keshava P. Singh was born in U.P., India where he obtained his B.E. degree in Electrical Engineering and Ph.D. in Plasma Physics from Banaras Hindu University. He is presently Reader in Electronics Engg. Department, I.T., B.H.U. His research area includes, Plasma Physics, Space Physics, Communication, Microwave Theory, Antenna Design and Remote Sensing. He has published 50 research papers in various Indian and foreign journals and 2 students obtained Ph.D. degree under his supervision.

Dr. Krishna K. Jha was born in Bihar, India and obtained his B.Sc. (Hons.) and M.Sc. degrees in Physics from Bihar University, Muzaffarpur in 1975 and 1977 respectively and the degree of Ph.D. for research in Microwave Remote Sensing in 1982 from Banaras Hindu University. He has published 18 scientific papers in various national and international journals. He is currently employed with Center of Research in Microwave Tubes, Dept. of Electronics Engg., I.T., B.H.U. His research area includes Remote Sensing, Electromagnetic Field Theory, Microwave Hardware and Theory and CAD of High Power Microwave Tube.

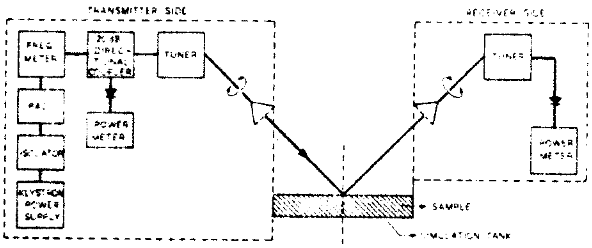

FIG. 1 - BLOCK DIAGRAM OF BISTATIC SCATTEROMETER SYSTEM

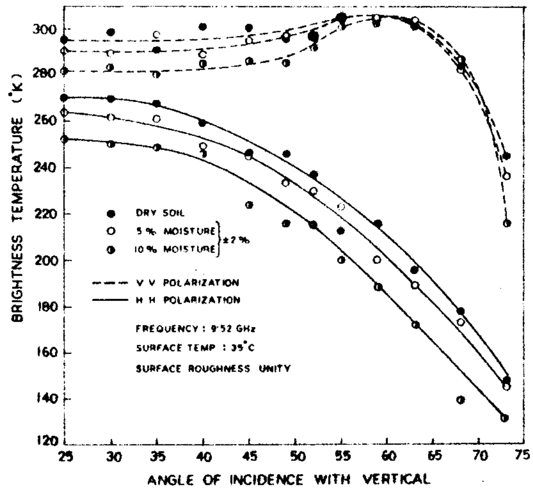

FIG. 2 - ANGULAR VARIATION OF BRIGHTNESS TEMPERATURE AS A FUNCTION OF MOISTURE CONTENT IN SOIL.

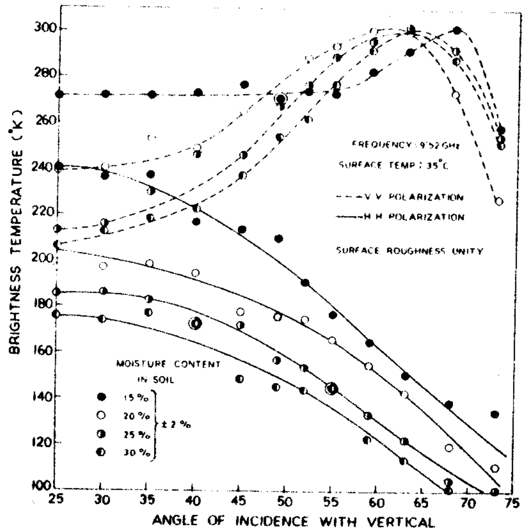

FIG. 3 - ANGULAR VARIATION OF BRIGHTNESS TEMPERATURE AS A FUNCTION OF MOISTURE CONTENT IN SOIL

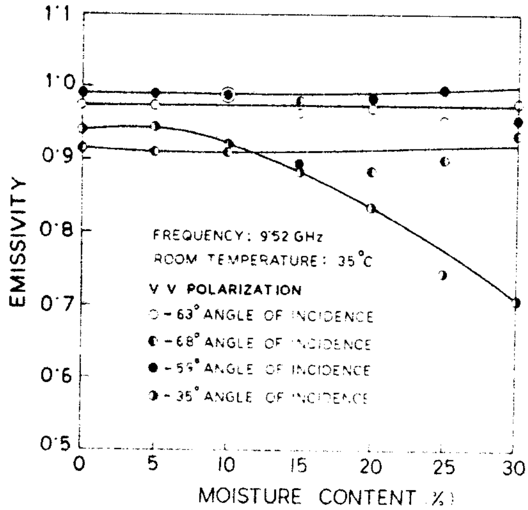

FIG. 4 - DEPENDENCE OF EMISSIVITY ON MOISTURE CONTENT AT ANGLES 35°, 59°, 63° & 68°.

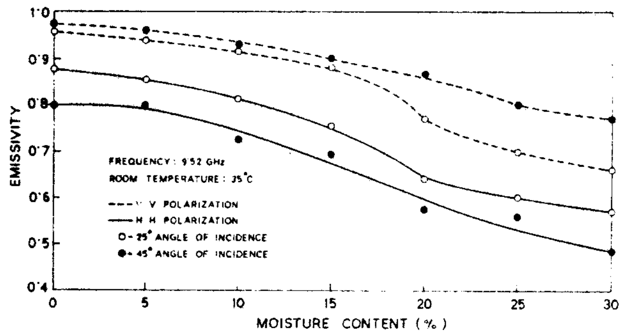

FIG. 5 - DEPENDENCE OF EMISSIVITY ON MOISTURE CONTENT AT ANGLES 25° AND 45°.

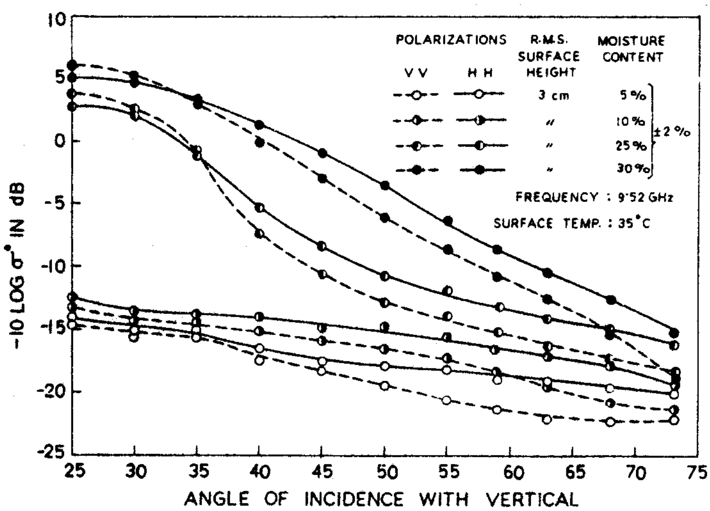

FIG. 6 - ANGULAR VARIATION OF SCATTERING COEFFICIENT (σ^0) AS A FUNCTION OF MOISTURE CONTENT AND SURFACE ROUGHNESS.

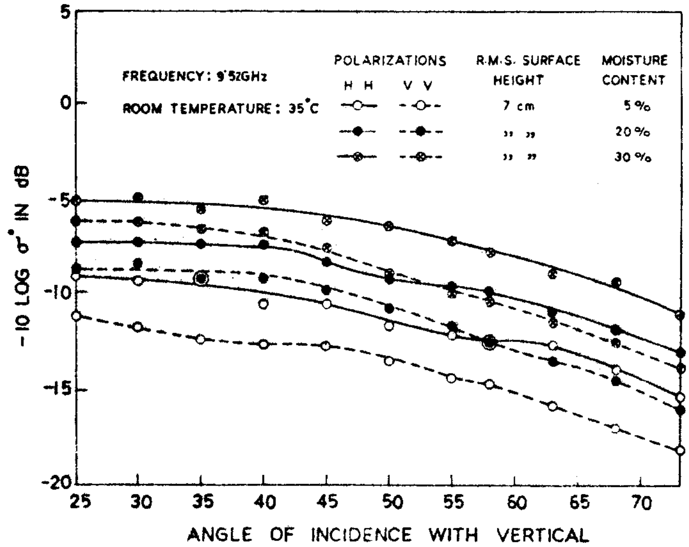

FIG. 7 - ANGULAR VARIATION OF SCATTERING COEFFICIENT (σ°) AS A FUNCTION OF MOISTURE CONTENT AND SURFACE ROUGHNESS.

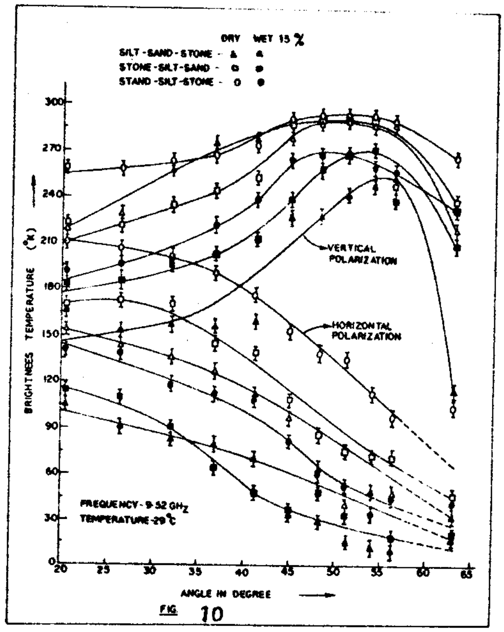

BRIGHTNESS TEMP. VARIATION WITH LOOK ANGLE.

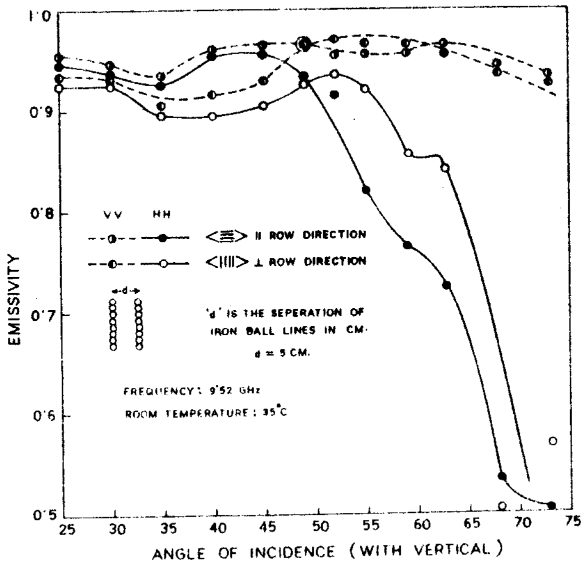

FIG. 8 - ANGULAR VARIATION OF EMISSIVITY FOR TWO CATAGORIES OF IRON BALL PATTERNS.

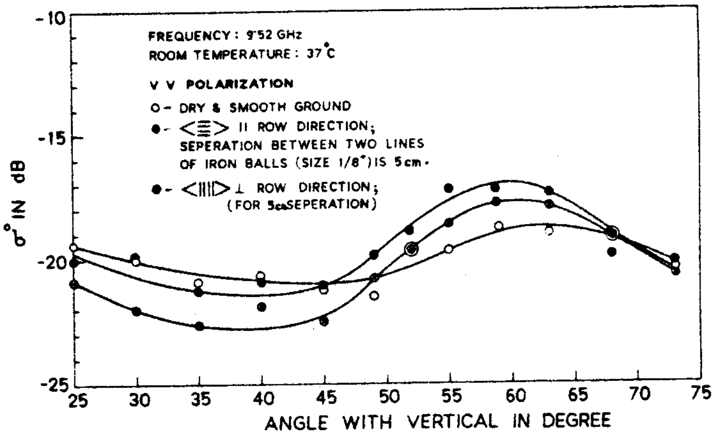

FIG. 9 - VARIATION OF BACK SCATTERING COEFFICIENT WITH ANGLE FOR TWO CATAGORIES OF IRON BALL PATTERNS.